Biogeosciences Discuss., 9, 14503–14535, 2012
www.biogeosciences-discuss.net/9/14503/2012/
doi:10.5194/bgd-9-14503-2012

Biogeosciences Discussions

Spatial and temporal aspects of greenhouse gas emissions from Three Gorges Reservoir, China

Y. Zhao, B. F. Wu, and Y. Zeng

Institute of Remote Sensing Applications, Chinese Academy of Sciences, Beijing, China

Received: 1 September 2012 – Accepted: 15 September 2012 – Published: 18 October 2012

Correspondence to: B. F. Wu (wubf@irsa.ac.cn)

Published by Copernicus Publications on behalf of the European Geosciences Union.

Abstract

Before completion of the Three Gorges Reservoir (TGR), China, there was growing apprehension that it would become a major emitter of greenhouse gases (GHG): Carbon Dioxide (CO_2), Methane (CH_4) and Nitrous Oxide (N_2O). We report monthly measurements for one year of the fluxes of these gases at multiple sites within the TGR, Yangtze River, China, and from several major tributaries, and immediately downstream of the dam. The tributary areas have lower CO_2 fluxes than the main storage; CH_4 fluxes to the atmosphere after passage through the turbines are negligible. Overall, TGR showed significantly lower CH_4 emission rates than most new reservoirs in temperate and tropical regions. We attribute this to the well-oxygenated deep water and high water velocities which produce oxic mainstem conditions inimical to CH_4 emission. TGR's CO_2 fluxes were lower than most tropical reservoirs and higher than most temperate systems. This is due to the high load of metabolizable soil carbon delivered through erosion to the Yangtze River. Compared to fossil fuelled power plants of equivalent power output TGR is a very small GHG emitter, annual CO_2-equivalent emissions are approximately 1.7 % of a coal-fired generating plant of comparable power output.

1 Introduction

The recently completed Three Gorges Reservoir on the Yangtze River, China, is one of the largest dams in the world. At full storage level (FSL = 175 m a.s.l.) it is 660 km long, decreasing to 556 km at planned lowest storage level of 145 m a.s.l in June each year, ready to receive flood waters. It has the largest installed power capacity and its annual power output is second in the world after Itaipu in Brazil. In addition to its hydropower capabilities TGR is important for flood control and navigation.

Since the start of construction there has been concern about the ecological impact of the reservoir (Giles, 2006; Stone, 2008; Qiu, 2009; Fu et al., 2010). An emerging element is the "greenness" of the electricity output. Reservoirs emit, to varying degrees,

BGD
9, 14503–14535, 2012

CO_2 and CH_4 arising from the metabolism of allochthonous and autochthonous organic matter (Louis et al., 2000). N_2O is emitted also. All these gases are radiatively active "greenhouse gases". While the CO_2 emissions have no net greenhouse impact as they are derived from photosynthetically fixed CO_2, the emissions of CH_4 and N_2O are especially important. Their relative molar atmospheric impacts are respectively 25 and 298 times that of CO_2 (Forster et al., 2007). It has been argued, based primarily on Brazilian hydro-reservoirs, that hydropower GHG emissions may be comparable to, or exceed those of, fossil-fuelled power stations of the same power capacity and thus vitiate their low GHG claims (Fearnside, 2002). This view is disputed (DosSantos et al., 2006). The latest consensus is that the relative GHG impact depends on the characteristics of the individual dam (Tremblay et al., 2005). TGR differs from the other well-studied boreal (Tremblay et al., 2005; Duchemin et al., 1995; Soumis et al., 2004) and tropical reservoirs (DosSantos et al., 2006; Guerin et al., 2006, 2008; Rosa et al., 2004) in a number of ways apart from its size:

- Physical configuration. The reservoir occupies a steep-sided gorge rather than a relatively shallow basin characteristic of the boreal and tropical reservoirs.
- Limited organic matter. Before inundation, 1.2 million people lived on the small and narrow riverine floodplain. They have been relocated and much of the vegetation and organic materials removed before the zone was flooded (Zhang et al., 2011). This situation is markedly different from the Brazilian case of flooded virgin rainforests.
- Major allochthonous organic C input is primarily particulate organic carbon (POC) associated with eroded soil (2.5 M tonnes C yr^{-1}) (Wu et al., 2007). This contrasts with boreal reservoirs where initial CO_2 emissions are driven by surface plant biomass and in the long term by sediment and pelagic respiration (Teodoru et al., 2011).

Against these background differences, our investigations of TGR have the objective of (1) evaluating the TGR GHG emissions and compare them to other hydro-reservoirs

BGD
9, 14503–14535, 2012

and other energy sources, (2) contributing (by providing data) to the development of an empirical model (Barros et al., 2011) to predict GHG emission from future reservoirs. Very recent research (Sobek et al., 2012; DelSontro et al., 2011) has shown that specific reservoir characteristics, not well reflected in some models, play a key role in high reservoir GHG emissions. Such models may play a role in future decisions on the construction of additional hydro-power reservoirs. It is important that they be robust, accurate and covers the widest range of circumstances. We address our results from this perspective later.

Despite their potential significance, there have only been limited investigations of the GHG emissions of TGR. Chen et al. (2009) reported relatively high emissions of CH_4 from stands of predominantly *Scirpus triqueter* ($14.9 \pm 10.9\,mg\,m^{-2}\,h^{-1}$) growing in temporary marshes formed in the drawdown zones of a tributary connected to the mainstem of TGR. Based on this observational data and, for the main body of the reservoir, an assumed emission rate of $3.3\,mg\,CH_4\,m^{-2}\,h^{-1}$ they concluded that the riparian zones constituted an important "hotspot" (about 20 % of total emissions from 10 % of the area). Subsequent measurements (no details provided) by the same group (Liu et al., 2011), in the main stem of TGR, drastically revised downward (factor of ~30) the previously assumed CH_4 emission rate in the TGR main stem. While this revision does not diminish the significance of the interfluvial zone for CH_4 emissions, it drastically reduces the total estimated CH_4 emissions by TGR, as the tributary area is much smaller than the main stem of the reservoir. Neither CO_2 nor N_2O fluxes were reported for the interfluvial zone.

2 Site characteristics

The Three Gorges Dam (Fig. 1) is located just upstream of Yichang (Hubei) on the mainstem of the Yangtze River. The principal source of the Yangtze is about 4500 km away on the Tibetan Plateau and the total catchment area above the dam is 1.1 million km^2. TGR is a typical valley-type reservoir with steep slopes on both sides of river

BGD
9, 14503–14535, 2012

channel. Geography of the reservoir catchment is complex with 74 % mountainous areas, only 4.3 % plain area in the river valley and 21.7 % hilly area. Annual average flow at Cuntan, the upstream end of the dam when full, is 11 100 cumecs. The area of the catchment directly between Cuntan and the dam is 58 000 km^2 and generates an additional annual average discharge to the Yangtze of 2800 cumecs. When the water level is 175 m a.s.l., the reservoir is about 1.1 km wide, with a total surface area of 1084 km^2 (782 km^2 mainstem and 302 km^2 tributary). Average depth of the reservoir is about 70 m and maximum depth in front of the Three Gorges Dam is about 170 m. The climate of the reservoir region is subtropical monsoon with an annual mean temperature of 18 °C. The river flow peak is in late summer coinciding with rains in the reservoir region. The local annual rainfall is about 1100 mm and occurs mainly from May to September.

Since the end of 2008, TGR has been in full operational mode: retaining water from late September until early November, the reservoir then runs at a high water level to late April in the following year. As the rainy season approaches, water level is drawn down gradually to 145 m, in preparation for flood retention and mitigation. The interplay between water inflows and outflows for power generation, flood control, facilitating navigation, and planned scouring of the bed sediment produces marked variations in the water residence times. These can be as short as 6 days at maximum design flows during the flood season and exceed 30 days in early summer when the dam is drawn down to its minimum level (145 m). The modeled water velocity in the upper mainstem (310 to 660 km from dam wall) remains above 2 $m\,s^{-1}$ irrespective of the dam level. In the 310 km stretch closest to the dam wall the modeled velocity is predicted to be about 0.5 $m\,s^{-1}$.

BGD
9, 14503–14535, 2012

3 Measurements

3.1 Field sites

Fluxes of CO_2, CH_4, and N_2O were measured monthly from January to December of 2010 at four primary sampling regions (Fig. 1). Zigui (ZG: just upstream of the dam wall, water depth 170 m at FSL), Badong (BD: 75 km upstream and depth 110 m at FSL) and Wanzhou (WZ: 282 km upstream and depth 80 m at FSL) are longitudinally distributed along the mainstem. Xiangxi (XX), the 4th primary site is on one of the biggest tributaries (Xiangxi River) in the reservoir region. Following the filling of TGR, the water velocity in the Xiangxi River decreased significantly and it is now a lake-like region prone to algal blooms (Ye et al., 2006, 2007). At each site 4–5 independent flux measurements were made each month to take into account the variability of gas emissions. Because of safety considerations all sampling sites were away from the central shipping channel, the water depth at all sites always exceeded 30 m.

In addition, GHG fluxes were measured at four supplementary regions further upstream (Zhutuo: ZT, Cuntan: CT, Longxi: LX, Qingxi: QX) and in two major tributaries (Xiaojiang: XJ and Daning: DN) inundated by the reservoir (Fig. 1). These regions cover a range of different environments with ZT above the reservoir influence. CT is in the interfluvial zone, formed as the reservoir water level is lowered from FSL to 145 m a.s.l., preparatory for the onset of the summer floods. All these sites were sampled monthly from June 2010 to May 2011.

Hydro-power reservoir GHG emissions occur not only through the surface of the reservoir but also by degassing downstream of the turbines. The extent of degassing depends on the precise conditions under which the water leaves the turbines. For instance in Petit Saut there is a hydraulic shute where the water is deflected into the air (Guerin et al., 2006). At TGR the water exits the turbines underwater and there is limited scope for immediate degassing. Two supplementary stations (Xiling Bridge: XLB and Huanglingmiao: HLM) below the dam were established specifically to quantify the degassing component of the GHG emissions. Surface CO_2 and CH_4 fluxes

BGD
9, 14503–14535, 2012

were measured at XLB in the turbulent dam tailrace 4.9 km downstream of the dam wall, and at HLM, 7 km downstream, in the tail waters of Gezhouba dam (about 38 km downstream) and at the edge of the less turbulent shipping channel.

3.2 Flux measurements

At each site CO_2, CH_4 and N_2O fluxes at the air-water interface were directly measured using floating static chambers, usually with two replicate chambers deployed at each sampling site. The chamber is a close-ended stainless steel cylinder, 60 cm in height and 30 cm in diameter, equipped with a dry battery driven fan and a small lateral vent sealed by silicon septum. The fans were turned on before the chambers were deployed, three air samples from each chamber were manually collected with 100 ml syringes at 0, 10, 20 min intervals (subsequently increased to 4 samples/30 min interval) after the deployment and stored in 500 ml air-tight gas sampling bags.

Gas samples were transported to the laboratory after field work and were analyzed by the Institute of Atmospheric Physics, Chinese Academy of Sciences. Gas concentrations were determined by a HP-4890D Gas Chromatograph (Agilent Corp.) according to the method described by Xing (2005). Gas standards were run before and after each set of samples in order to check reproducibility of results and to evaluate the precision of measurements. The detection limit of the gas chromatograph is 0.1 ppm and the minimum detectable flux is 0.1 $mg\,m^{-2}\,d^{-1}$, with analytical error on duplicate standard samples of less than 1 %. Gas flux was calculated from a linear regression with gas concentration change within chamber versus time (IHA, 2010):

$$\text{Flux}\,(\text{mg}\,\text{m}^{-2}\,\text{d}^{-1}) = \frac{\text{Slope}\,(\text{ppm}\,\text{s}^{-1}) \times F_1 \times F_2 \times \text{ChambleVolume}\,(\text{m}^3)}{\text{ChamberSurface}\,(\text{m}^2)} \quad (1)$$

Where slope is the value from linear regression of the gas concentration change within the chamber versus time, F_1 is a conversion factor from ppm to $mg\,m^{-3}$ for standard temperature and pressure for gas in air and F_2 is a conversion factor of seconds into

BGD
9, 14503–14535, 2012

days. Only the sites where the gas concentration change had a linear regression coefficient over 0.8 were included in the calculation.

3.3 Water environment sampling

While collecting air samples, the temperature inside the chamber, air temperature, and water temperature were measured with a JM624 portable digital thermometer equipped with 6 m length probes. Water conductivity, and Dissolved Oxygen (DO) were measured in-situ (depth = 0.5 m) with a DDB-3 (Leici Instrument, Shanghai, China) and a JPB-607 DO meter (Leici Instrument, Shanghai, China) respectively, transparency was determined using Secchi disk. Water samples at 0.5 m depth were collected for laboratory analysis of chlorophyll *a*, turbidity, total phosphorous (TP), total nitrogen (TN) and total organic carbon (TOC). The analysis of the water samples were performed by the Institute of Hydrobiology, Chinese Academy of Sciences (Yang et al., 2011).

Water column physic-chemical data was provided by the Bureau of Hydrology, Changjiang Water Resources Commission. Vertical profiles of water temperature and DO concentrations were measured monthly in front of the dam from July 2008 to June 2009. Water temperature was measured at 2 m intervals from top to the bottom of the reservoir, using the reversing thermometer method (according to national standard: water quality – determination of water temperature – thermometer or reversing thermometer method, GB 13195-91), while DO concentrations were sampled at the surface (0.5 m), bottom and middle layer using Winkler titration method (according to national standard: water quality – determination of dissolved oxygen – iodometric method, GB 7489-87).

3.4 Data analysis and total areal emission calculation

Mean CO_2, CH_4 and N_2O fluxes were calculated by averaging the available replicate samplings in each region. The results were used to compare the fluxes between different regions directly. To calculate the total GHG emissions from the TGR, we divided

BGD
9, 14503–14535, 2012

the water surface into 25 subregions (11 mainstem regions and 15 tributary regions), reflecting the boundaries between mainstream and tributary areas and administrative boundaries. Areas of each subregion under water level of 135, 145, 156 and 175 m were extracted using a 10 m resolution digital precision elevation map (DEM). Linear relationships between water level and surface water area for each subregion were then established using a regression analysis and the surface area at different water level was calculated. Subregions without measured flux were interpolated using the values of the two nearest regions.

Arcgis 9.3 was used to manipulate the DEM while other above analysis was performed with the EXCEL 2007 software. GHG emissions from the TGR were calculated by multiplying the total averaged CO_2 fluxes from the sampling regions each month by the surface water area, CH_4 emissions were added up to the total emission by multiply its Global Warming Potential value (GWP: 25). Equivalent CO_2 emission per unit generating capacity was further calculated by dividing by the power generation of the TGR. Meanwhile, CO_2 and CH_4 emissions were related to water quality variables by Pearson correlation analysis, which was performed with SPSS 16.0 software.

4 Results

4.1 Spatial and temporal variation of CO_2 fluxes

The results (Fig. 2) show that the surface waters at mainstem stations (WZ, BD, and ZG), are sources of CO_2 to the atmosphere all year round with the CO_2 fluxes higher in warm season (Fig. 5). This is the period with high flow also. The fluxes at the 3 primary mainstem stations were consistently high (WZ, $126 \pm 110\,\mathrm{mmol\,m^{-2}\,d^{-1}}$; BD, 126 ± 80; and ZG, $104 \pm 87\,\mathrm{mmol\,m^{-2}\,d^{-1}}$). While the annual average CO_2 fluxes at the upstream regions varied. The fluxes are less at upstream ZT ($88 \pm 57\,\mathrm{mmol\,m^{-2}\,d^{-1}}$) and comparable to those at the 3 mainstem stations at QX ($127 \pm 57\,\mathrm{mmol\,m^{-2}\,d^{-1}}$), CT ($170 \pm 97\,\mathrm{mmol\,m^{-2}\,d^{-1}}$) and LX ($175 \pm 150\,\mathrm{mmol\,m^{-2}\,d^{-1}}$). Overall the CO_2 fluxes

BGD
9, 14503–14535, 2012

at mainstem regions are higher during the rainy season. This finding suggests that CO_2 production is due to the oxidation of incoming particulate organic carbon from the catchment, primarily soil organic carbon (Wu et al., 2007). Relative to ZT (the representative upstream riverine site, i.e. unimpacted by the full reservoir waters), average mainstream CO_2 fluxes have increased by 56 %.

The tributary region at XX shows markedly contrasting behavior (Fig. 5). The CO_2 flux was negative (i.e. from the atmosphere into the water) during the summer, due to photosynthetic uptake by phytoplankton, and is consistent with the very high chlorophyll *a* concentrations recorded there, and a higher transparency compared to other regions. Because of the photosynthetic uptake there the Xiangxi River has the lowest average annual CO_2 flux ($25 \pm 54\,mmol\,m^{-2}\,d^{-1}$). The CO_2 fluxes at the tributary regions were less than all the mainstem regions (XJ $79 \pm 52\,mmol\,m^{-2}\,d^{-1}$; DN $25 \pm 30\,mmol\,m^{-2}\,d^{-1}$), 50.6 % less than reference (ZT). All the tributary regions have a large standard error (Fig. 2) reflecting a substantial seasonal variation of CO_2 due to drawdown by photosynthesis during the summer season with still shallower waters favoring pelagic phytoplankton, and submerged and emergent vegetation growth leading to low CO_2 fluxes. This stock of organic matter is subsequently submerged and oxidized during the high water stage leading to high CO_2 fluxes post-TGR reaching its full operational level.

The annual average CO_2 fluxes from the downstream station closer to the dam wall (XLB: $81 \pm 80\,mmol\,m^{-2}\,d^{-1}$) is less (though not statistically significant) than that at ZG immediately upstream of the dam wall. The difference of $23\,mmol\,m^{-1}\,d^{-1}$ suggests that about 22 % of CO_2 degassed due to the turbulence induced after the power house, this is comparable to rapids in a river, like ZT in this research. This is also partly approved by the higher results of HLM ($212 \pm 136\,mmol\,m^{-2}\,d^{-1}$), the station which only 2 km further downstream.

BGD
9, 14503–14535, 2012

4.2 Spatial and temporal variation of CH_4 and N_2O fluxes

The four primary regions (ZG, BD, WZ, and XX) act, at times, as both sources and weak sinks of CH_4 (Fig. 5). Yearly averaged flux at XX was $0.41 \pm 0.96\,mmol\,m^{-2}\,d^{-1}$, higher (though not statistically significant) than the other three regions excluding the peak value of $3.12\,mmol\,m^{-2}\,d^{-1}$ in June in WZ. This high value was thought to be caused by the sudden rain at the sampling site, and the combined effects of shallow water and disturbances by passing ships. Consequently, WZ has the highest CH_4 flux among the three mainstream regions, with an averaged flux of 0.76 ± 1.11, and $0.40 \pm 0.52\,mmol\,m^{-2}\,d^{-1}$ after excluding the June value. The values for BD and ZG are 0.09 ± 0.33 and $0.04 \pm 0.46\,mmol\,m^{-2}\,d^{-1}$, respectively. Upstream, reservoir tail waters (CT, LX and QX) and tributary stations had relative higher CH_4 fluxes than the main stem of the reservoir (Fig. 2), reflecting the greater autochthonous production in these areas as well as the greater deposition of reactive particulate organic matter entering TGR in these zones. Again, relative to ZT, the mainstem area had 59 % lower CH_4 flux and tributary area had 65 % less. The general principle seems that "the deeper site, the lower the CH_4 flux". The annual average CH_4 fluxes (Fig. 2) from the 2 downstream stations (XLB $0.17\,mmol\,m^{-2}\,d^{-1}$ and HLM $0.53\,mmol\,m^{-2}\,d^{-1}$) are slightly higher than fluxes at ZG immediately above the dam wall. The water CH_4 concentrations are not significantly different suggesting that the losses through the turbines are limited and that the flux differences arise from much higher turbulence in the zone immediately downstream of the dam (Vachon et al., 2010).

N_2O fluxes were much lower compared to CO_2 and CH_4 fluxes (Fig. 4), the total average fluxes at the mainstream and Xiangxi River were 0.01 ± 0.01 and $0.004 \pm 0.01\,mmol\,m^{-2}\,d^{-1}$, respectively, consistent with the suggestion of very small N_2O fluxes from freshwater reservoirs (Huttunen et al., 2003). Even after conversion to equivalent GHG fluxes (×298) the N_2O contribution to total reservoir GHG flux is negligible.

BGD
9, 14503–14535, 2012

4.3 Water environment dynamics

As demonstrated in Fig. 6, TGR had slightly basic waters (mean pH: 8.04, Fig. 6b). The temperature of the surface water varies according to the regional climate and there were no significant differences between the four sampling water regions (Fig. 6a) chlorophyll *a* concentration was relatively low from January to February and October to December in the TGR. In remaining months, chlorophyll *a* concentration in Xiangxi River was much higher than in the mainstream and it recorded a peak value of 40.46 $\mu g l^{-1}$ in June (Fig. 6c). As an index of balance between photosynthesis and respiration, dissolved oxygen in surface water was influenced by the activity of algae and showed a similar spatial-temporal variation type to the chlorophyll *a* concentration (Fig. 6d). Transparency (Secchi depth) reflected the content of suspended sediments low values occurred during the rainy season (from May to September), mainly due to the input of terrestrial solids brought by the surface runoff in the drainage basin (Fig. 6e). TOC in the TGR was relatively low for most of the sampling period but rose during the rainy season (Fig. 6f).

The water temperature (Fig. 7) undergoes an annual cycle between 11.4 °C and 25.5 °C. Only in April and May is there substantial temperature stratification but this always occurs below the turbine offtake level (116 m above the dam floor).Meanwhile, DO concentrations (Fig. 8) measured at different depths show that the complete water column has high DO concentrations (> 6 $mg l^{-1}$) everywhere. The water column of the reservoir is well mixed top to bottom for most of the year and we attribute this to the high flows/short residence time caused by the generally highflows required for maximum power generation.

BGD
9, 14503–14535, 2012

5 Discussion

5.1 Mechanisms of GHG fluxes

To gain insights into the possible mechanisms controlling fluxes, we examined the correlations between the measured fluxes of CO_2 and CH_4 and other environmental parameters measured at those sites (Table 1). There is a strong negative correlation ($R = -0.368$, $p < 0.001$) between CO_2 flux and chlorophyll *a*, suggesting that photosynthetic uptake of CO_2 reduces the net flux. This conclusion is consistent with the temporal trends observed, with the chlorophyll *a* concentration reaching a maximum at summer low water when the water transparency was a maximum and the tributary water velocities lowest (Fig. 6). Station XX is one of the tributary regions now prone to algal blooms post-dam completion due to the dramatically reduced current velocity and an abundance of nutrients, The strong negative correlation between DO and CO_2 fluxes also is consistent with the influence of algal photosynthesis processes on CO_2 fluxes, as O_2 is produced simultaneously by the same processes which are removing CO_2.

The observed negative correlation between transparency and CO_2 fluxes ($r = -0.261$, $p = 0.001$) reflects the key role of allochthonous POC in reservoir CO_2 production, especially at the three mainstream sampling regions. Low transparency (<1 m) occurs from May to September (Fig. 6), when major inflows as well as rainfall events happens in the region. The input of particles from the drainage basin through surface runoff decreases the transparency, but increases both dissolved and particulate allochthonous carbon (Oelbemann et al., 2011) These sources of degradable organic carbon enhance CO_2 production, despite the dilution effects of the higher flows. Similar findings were noted in several lakes and reservoirs in Finland (Huttunen et al., 2003), where the authors observed that both the autochthonous and allochthonous carbon sources were important in the GHG emissions from reservoirs. This result confirms earlier work suggesting that freshwater lakes, rivers and reservoirs play a major role in the transfer of terrestrially fixed carbon to the atmosphere, although they account for

BGD
9, 14503–14535, 2012

less than 0.4 percent of the earth's surface (Tremblay et al., 2005). Water temperature plays an important role in these processes also. Higher water temperature during the period results in higher rates of decomposition of organic carbon, and this temperature dependence explains also why CO_2 fluxes were much lower in colder seasons.

None of the analyzed variables showed high correlation with air-water interface CH_4 fluxes. Chlorophyll *a* was related however to CH_4 fluxes with a high significance ($p < 0.01$). This is consistent with much of the autochthonous production contributing to the formation of sediment anoxia due to the highly reactive phytoplankton detritus leading to conditions appropriate for CH_4 production. Earlier work noted that in eutrophic reservoirs with anoxic hypolimnion a large amount of organic carbon fixed by photosynthesis was recycled as CH_4 (Tremblay et al., 2005).

The drawdown zone of a reservoir is generally considered to be a "hot spot" for CH_4 emissions (Bergstrom et al., 2007). Clearly it forms a quasi-littoral zone where riparian vegetation growth can occur and organic-rich sediment is deposited. On refilling, microbial metabolism of the organic carbon plus reduced oxygen supply leads to anoxic sediments and production of CH_4. The potential littoral zone of the main stem of TGR is quite limited due to the steep-sided configuration. The largest quasi-littoral zone in the TGR forms along the tributaries with a smaller zone extending along the edges of the mainstem as the water is progressively drawn down. CH_4 fluxes will rise in the still wetted regions here as water shallows, however, much of this area is scoured out during the first major flood event and CH_4 fluxes then fall back to closer to those elsewhere in the main stem (Fig. 2). The tributaries, on the other hand, are less subject to scouring, as the power of the tributary remains the same, while the area of the wetted zone subject to drawdown is increased due to the raised water level. Thus, in the tributaries the draw down area takes on much of the character of a quasi-permanent littoral deposition zone with continuing accumulation of organic rich sediments occurring over repeated reservoir emptying and filling cycles. This conceptual description explains the phenomenon described by Bergstrom et al. (2007) and the high CH_4 fluxes observed by us in these zones (XJ, DN, and XX) and previously reported in another TGR tributary

BGD
9, 14503–14535, 2012

by Chen et al. (2009). The CH_4 fluxes we measured at these tributary sites are considerably less, however, than those reported by Chen et al. (10.05 mmol m^{-2} d^{-1}). We conclude that littoral CH_4 fluxes are highly spatially variable and that caution needs to be exercised in extrapolating these fluxes to the reservoir as whole, or even to the total littoral area as done by Qiu (2009).

The seasonally changing differences over time in flux behavior in the different spatial elements especially the tributaries and inter fluvial areas of the TGR underlines the need for a spatially and temporally representative sampling of gas fluxes, as relatively small areas can have a disproportionate effect on total emissions. Specific operational factors (water depth, high oxygen content due to the turbulent conditions, and short residence time) cause TGR to fall well outside the predictions of CH_4 emissions with age (Barros et al., 2011). Based on the age and latitude of TGR CO_2 fluxes are underpredicted while CH_4 fluxes are over predicted. The existence of other systems such as Lake Wohlen (DelSontro et al., 2011) which depart significantly from such predictions also, suggests that a more nuanced approach is needed in predicting GHG emissions from hydropower reservoirs.

5.2 Comparison with other reservoirs and other energy sources

The total area weighted average emission from the TGR (normalized by installed capacity) was 4.63 mol kWh^{-1} d^{-1} and 0.02 mol kWh^{-1} d^{-1} for CH_4. Compared with other storages (Table 2), TGR showed significantly lower CH_4 emissions than most new reservoirs in temperate and tropical regions. We attribute this to less inundated biomass, and deep well-mixed, and oxygenated water in TGR. CO_2 emissions were higher than most temperate reservoirs but still lower than most tropical reservoirs. This arises from the high carbon load delivered to TGR. The Yangtze River system had higher organic content and exports more organic carbon than some comparable large rivers such as Mississippi, but less than that of the Amazon River (Wu et al., 2007).

In 2010, TGR emitted about 1.3×10^6 t CO_2, 6×10^3 t CH_4 and 128 t N_2O from the reservoir surface. Taking account of the global warming potential of CH_4 and N_2O,

BGD
9, 14503–14535, 2012

the annual emission of CO_2 equivalents was estimated to be 1.5×10^6 t. In 2010, the Three Gorges power station generated a total of 8.437×10^{10} kWh. Thus TGR will emit $17.88\,g\,CO_{2equiv}\,kWh^{-1}$, which means $4.8 \times 10^{-3}\,t\,C\,MWh^{-1}$. The equivalent emissions produced by thermal power plants burning different fuels such as coal, fuel oil, natural gas with different technology efficiency levels were calculated using emission factors from the IPCC Emission Factor Database (Table 3). Total GHG emissions from TGR were much lower than the annual CO_2 emissions from other power sources (1.7 % of coal, and 3.9 % of natural gas).

5.3 Uncertainties

As noted earlier we focus on gross surface fluxes here and do not differentiate between diffusive and bubble fluxes. It is possible, however, to infer from the number of discontinuities in the individual plots of the chamber measurements when a bubble (or a series of bubbles) has entered the measuring chamber. These bubble events are most frequent at tributary sites and occur mainly in summer consistent with the previously observed effects of declining pressure stimulating bubble emissions, as well as reduced gas transfer from the rising bubble to the surrounding water (McGinnis et al., 2006), as well as the enhanced CH_4 production in the sediments due to the higher temperatures. This conclusion is similar with other research that bubble emissions are a major component of the total flux under particular conditions: in dendritic reservoirs with substantial vegetated littoral zones, shallow deltaic deposition zones (DelSontro et al., 2011; Chen et al., 2009) coupled with shallow depths (McGinnis et al., 2006). So this work deals with the gross fluxes only as this is the key measurement determining the "greenhouse" impact, a recent research. More detailed investigation of the bubble fluxes is now underway.

Our approach overestimates the actual GHG impact of the TGR as we do not take account of river emissions before formation of the impoundment. The pre-impoundment GHG emissions must be subtracted from our measured emissions to calculate the net

BGD
9, 14503–14535, 2012

GHG emissions, i.e. the extra emissions attributable to the dam. In our study of TGR, we don't have the requisite flux data before the dam construction. We overcome this gap using the IHA method (IHA, 2010). Here we use an upstream region such as Zhutuo (ZT), which is unaffected or less affected by reservoir backwater, as a reference, and examine the differences between the reference and the dam-affected sites further downstream.

Comparing the annual average flux from ZT with those of the other regions we see that the main stem regions and the regions below the dam have marginally increased CO_2 emission. We attribute this increase to the construction and operation of the reservoir. All the tributary regions, however, have reduced CO_2 emissions compared to upstream regions. In those tributary regions, the impoundment has converted a rapidly flowing narrowly confined river into broader, quieter backwater with enhanced uptake of CO_2 by riparian vegetation and phytoplankton thus reducing the overall net CO_2 flux especially during spring and summer. During the high flow events much of this material is swept downstream and its subsequent conversion to CO_2 is attributed to the zone of its metabolism rather than to area where the CO_2 was fixed. On the whole, if we don't consider the area change of surface water before and after the dam construction, a estimate amount of 1.1×10^6 t CO_2 would be emitted without impoundment, which indicated CO_2 emission have increased by 17.5 % due to the impoundment.

The situation is different for CH_4 emissions. Relative to our upstream reference regions, we see that CH_4 emissions from the main stem are significantly lower ($p = 0.001$). The value before the dam construction was estimated to be 16.1×10^3 t, which means CH_4 emissions have decreased by 62.8 %. Emission of CH_4 is contingent on the creation of anoxic zones within the sediments and the absence of other factors limiting CH_4 emissions from the surface. These limiting factors include an oxygenated water column where oxidation of dissolved CH_4 may occur (Bastviken et al., 2006), and deep waters promoting the dissolution of CH_4 bubbles thus reducing the "direct" bubble flux to the surface and prolonging the time dissolved CH_4 is exposed to oxidation in the water column (McGinnis et al., 2006). The high DO concentrations even in

BGD
9, 14503–14535, 2012

the deepest parts of the TGR storage minimize the scope for sediment anoxia. The great water depth favors dissolution of the bubbles emitted from the sediment before they reach the surface. Thus the surface emission of CH_4 is confined largely to diffusive fluxes. It is interesting to note that the inferred highest incidence of bubbles at the surface corresponds to the time of the summer drawdown with the warmest and most shallow waters. The upstream and tributary stations CH_4 emissions are significantly increased (p = 0.001 and 0.083, for upstream and tributary, respectively) reflecting the increased scope for sedimentation in these areas, and for autochthonous production which contributes to the formation of the anoxic zones.

6 Conclusions

Our results answer concerning questions about the GHG impact of TGR as well as increasing knowledge of the processes controlling GHG fluxes from reservoirs. Compared to fossil-fuelled power plants of equivalent power output TGR is a very small GHG emitter. Relative to other hydroplants TGR's outputs of CH_4 and CO_2 per unit of generating capacity are comparable to temperate hydropower plants but considerably less than emissions from tropical hydrosystems.

The construction of the dam has led to a marginal increase in the mainstem CO_2 fluxes. These are already high due to the high load of metabolizable soil carbon delivered by erosion to the Yangtze. The tributaries and increased interfluvial areas formed on damming, and the operations of the dam have become more favourable to photosynthetic uptake of CO_2 especially in summer. While this reduces the measured annual average CO_2 fluxes, however it is likely that some of this material will be converted back to CO_2 elsewhere diminishing any net effect.

The post dam construction conditions in these tributary areas however, have lead to increased CH_4 fluxes in the tributaries and the interfluvial zone upstream compared to the pre-dam state. In the main body of the reservoir, the great depth of the water column, the lack of stratification and the high oxygen content of the water column limit CH_4

BGD
9, 14503–14535, 2012

fluxes by providing sufficient depth for all bubbles to dissolve (McGinnis et al., 2006) before reaching the surface preventing ebullitive delivery of CH_4 to the atmosphere. Dissolved CH_4 is rapidly oxidized limiting diffusive emissions.

The seasonally changing differences over time in emission behavior in the different spatial elements especially the tributaries and inter fluvial areas of the TGR underlines the need for a spatially and temporally representative sampling of gas emissions, as relatively small areas can have a disproportionate effect on total emissions. The operation of specific factors (depth, high oxygen content due to the turbulent conditions, and short residence time) cause TGR to fall well outside the predictions of CH_4 emissions with age (Barros et al., 2011). Based on the age and latitude of TGR CO_2 fluxes are under-predicted while CH_4 fluxes are over predicted. The existence of other systems such as Lake Wohlen (DelSontro et al., 2011) which depart significantly from such predictions also, suggests that a more nuanced approach is needed in predicting GHG emissions from hydropower reservoirs.

Acknowledgements. This research was jointly supported by the Major State Basic Research Development Program of China (973 Program) (No.2010CB955904) and Knowledge Innovation Program of the Chinese Academy of Sciences (No. ZNWH-2011-014). We appreciate support from Zhiqiang Zhou, and Chao Yuan for participation in the field campaign. We also appreciate Xiaoke Wang, Yuchun Wang, Yonghong Bi, Shangbin Xiao, Jinsong Guo providing field data. We thank P.W. Ford (CSIRO, Australia) for editorial assistance.

References

Barros, N., Cole, J. J., Tranvik, L. J., Prairie, Y. T., Bastviken, D., Huszar, V. L. M., Giorgio, P. D., and Roland, F.: Carbon emission from hydroelectric reservoirs linked to reservoir age and latitude, Nat Geosci., 4, 593–596, 2011.

Bastviken, D., Ljlertsson, J., and Tranvik, L.: Measurement of methane oxidation in lakes: a comparison of methods, Environ, Sci. Technol., 36, 3354–3361, 2006.

BGD

9, 14503–14535, 2012

Bergstrom, I., Makela, S., Kankaala, P., and Kortelainen, P.: Methane efflux from littoral vegetation stands of southern boreal lakes: an upscaled regional estimate, Atmos. Environ., 41, 339–351, 2007.
Chen, H., Wu, Y., Yuan, X., Gao, Y., Wu, N., and Zhu, D.: Methane emissions from newly created marshes in the drawdown area of the Three Gorges Reservoir, J. Geophys. Res., 114, D18301, doi:10.1029/2009JD012410, 2009.
DelSontro, T., Kunz, M. J., Kempter, T., Wüest, A., Wehrli, B., and Senn, D. B.: Spatial heterogeneity of methane ebullition in a large tropical reservoir, Environ. Sci. Technol., 45, 9866–9873, 2011.
DosSantos, M. A., Rosa, L. P., Sikar, B., Sikar, E., and DosSantos, E. O.: Gross greenhouse gas fluxes from hydro-power reservoir compared to thermo-power plants, Energ. Policy, 34, 481–488,2006.
Duchemin, E., Lucotte, M., Canuel, R., and Chamberland, A.: Production of the greenhouse gases CH_4 and CO_2 by hydroelectric reservoir of the boreal region, Global Biogeochem. Cy., 9, 529–540, 1995.
Fearnside, P. M.: Greenhouse gas emissions from a hydroelectric reservoir (Brazil's Tucurui Dam) and the energy policy implications, Water Air Soil Pollut., 133, 69–96, 2002.
Forster, P., Ramaswamy, V., Artaxo, P., Berntsen, T., Betts, R., Fahey, D. W., Haywood, J., Lean, J., Lowe, D. C., Myhre, G., Nganga, J., Prinn, R., Raga, G., Schulz, M., and Dorland, R. V.: Changes in atmospheric constituents and in radiative forcing, in: Climate Change 2007: The Physical Science Basis. Contribution of Working Group I to the Fourth Assessment Report of the Intergovernmental Panel on Climate Change, Cambridge Univ. Press, Cambridge, UK and New York, NY, USA, 212, 2007.
Fu, B. J., Wu, B. F., Lu, Y. H., Xu, Z. H., Cao, J. H., Niu, D., Yang, G. S., and Zhou, Y. M.: Three Gorges project: efforts and challenges for the environment, Prog. Phys. Geogr., 34, 741–754, 2010.
Giles, J.: Methane quashes green credentials of hydropower, Nature, 444, 524–525, 2006.
Graus, W. H. J., Voogt, M., and Worrell, E.: International comparison of energy efficiency of fossil power generation, Energ. Policy, 35, 3936–3951, 2007.
Guerin, F., Abril, G., and Richard, S.: Methane and carbon dioxide emissions from tropical reservoirs: significance of downstream rivers, Geophys. Res. Lett., 33, L21407, doi:10.1029/2006GL027929, 2006.

BGD
9, 14503–14535, 2012

Guerin, F., Abril, G., de Junet, A., and Bonnet, M.: Anaerobic decomposition of tropical soils and plant material: implication for the CO_2 and CH_4 budget of the Petit Saut Reservoir, Appl. Geochem., 23, 2272–2283, 2008.

Huttunen, J. T., Alm, J., Liikanena, A., Juutinen, S., Larmola, T., Hammar, T., Silvola, J., and Martikainen, P. J.: Fluxes of methane, carbon dioxide and nitrous oxide in boreal lakes and potential anthropogenic effects on the aquatic greenhouse gas emissions, Chemsosphere, 52, 609–621, 2003.

International Hydropower Association: GHG measurement guidelines for freshwater reservoirs, Sutton, London, 2010.

Liu, L., Chen, H., Yuan, X. Z., Chen, Z. L., and Wu, Y. Y.: Unexpected CH_4 emission from the Three Gorges Reservoir and its implications, Ac. Ecol. Sin., 31, 233–234, 2011.

Louis, V. L. S., Kelly, C. A., Duchemin, E., Rudd, J. W. M., and Rosenberg, D. M.: Reservoir surfaces as sources of greenhouse gases to the atmosphere: a global estimate, Bioscience, 50, 766–775, 2000.

McGinnis, D. F., Greinert, J., Artemov, Y., and Wüest, A.: Fate of rising methane bubbles in stratified waters: how much methane reaches the atmosphere? J. Geophys. Res., 111, C09007, doi:10.1029/2005JC003183, 2006.

Oelbermann, M. and Schiff, S. L.: The redistribution of soil organic carbon and nitrogen and greenhouse gas production production rates during reservoir drawdown and reflooding, Soil Sci., 175, 72–80, 2011.

Qiu, J.: Chinese dam may be a methane menace, Nature, doi:10.1038/news.2009.962, 2009.

Rosa, L. P., DosSantos, A. M., Matvienko, B., DosSantos, E. O., and Sikar, E.: Greenhouse gas emissions from hydroelectric reservoirs in tropical regions, Clim. Change, 66, 9–21, 2004.

Sobek, S., DelSontro, T., Wongfun, N., and Wehrli, B.: Extreme organic carbon burial fuels intense methane bubbling in a temperate reservoir, Geophys. Res. Lett., 39, L0141, doi:10.1029/2010GL050144, 2012.

Soumis, N., Duchemin, E., and Lucotte, R. C. A. M.: Greenhouse gas emissions from reservoirs of Western United States, Global Biogeochem. Cy., 18, GB3022, doi:10.1029/2003GB002197, 2004.

Stone, R.: Three Gorges Dam: into the unknown, Science, 321, 628–632, 2008.

Teodoru, C. R., Prairie, Y. T., and Giorgio, P. A. D.: Spatial heterogeneity of surface CO_2 fluxes in a newly created Eastmain-1 reservoir in Northern Quebec, Canad. Ecosystems, 14, 28–46, 2011.

BGD
9, 14503–14535, 2012

Tremblay, A., Varfalvy, L., Roehm, C., and Garneau, M. (Eds.): Greenhouse Gas Emissions – Fluxes and Processes: Hydroelectric reservoirs and natural environments, Environmental Science Series, Springer, New York, 2005.

Vachon, D., Prairie, Y. T., and Cole, J. J.: The relationship between near-surface turbulence and gas transfer velocity in freshwater systems and its implications for floating chamber measurements of gas exchange, Limnol. Oceanogr., 55, 1723–1732, 2010.

Wu, Y., Zhang, J., Liu, S. M., Zhang, Z. F., Yao, Q. Z., Hong, G. H., and Cooper, L.: Sources and distribution of carbon within the Yangtze River system, Estuar. Coastal Shelf Sci., 71, 13–25, 2007.

Xing, Y., Xie, P., Yang, H., Ni, L., Wang, Y., and Rong, K.: Methane and carbon dioxide fluxes from a shallow hypereutrophic subtropical lake in China, Atmos. Environ., 39, 5532–5540, 2005.

Yang, M., Bi, Y. H., Hu, J. L., Zhu, K. X., Zhou, G. J., and Hu, Z. Y.: Seasonal variation in functional phytoplankton groups in Xiangxi Bay, Three Gorges Reservoir, Chin. J. Oceanol. Limn., 29, 1057–1064, 2011.

Ye, L., Xu, Y. Y., and Han, X. Q.: Daily dynamics of nutrients and chlorophyll *a* during a spring phytoplankton bloom in Xiangxi Bay of the Three Gorges Reservoir, J. Freshwater Ecol., 21, 315–321, 2006.

Ye, L., Han, X. Q., Xu, Y. Y., and Cai, Q. H.: Spatial analysis for spring bloom and nutrient limitation in Xiangxi bay of Three Gorges Reservoir, Environ. Monit. Assess., 127, 135–145, 2007.

Zhang, Q. and Lou, Z.: The environmental changes and mitigation actions in the Three Gorges Reservoir region, China, Environ. Sci. Policy, 14, 1132–1138, 2011.

BGD

9, 14503–14535, 2012

Table 1. Correlation between CO_2 and CH_4 fluxes and measured variables, surface water (0.5 m) of TGR.

	Tw (°C)	SD (cm)	chl *a* ($\mu g l^{-1}$)	pH	DO ($mg l^{-1}$)	turb (NTU)	TOC
CO_2	0.142	−0.261[2]	−0.368[2]	−0.148	−0.369[2]	0.241[2]	0.116
CH_4	0.063	−0.145	0.237[2]	0.048	0.260[2]	−0.041	−0.170[1]
N_2O	0.054	−0.245[2]	−0.034	−0.038	−0.294[2]	0.303[2]	0.228[2]

[1] Correlation is significant at the 0.05 level.
[2] Correlation is significant at the 0.01 level.

BGD
9, 14503–14535, 2012

Table 2. CO_2 and CH_4 emissions of per unit installed power generation capacity.

Reservoir	Location	Cimate	Area km^2	Installed Capacity MW	CO_2 fluxes $mmol\,m^{-2}\,d^{-1}$	CH_4 fluxes $mmol\,m^{-2}\,d^{-1}$	CO_2 emission $mol\,kWh^{-1}\,d^{-1}$	CH_4 emission $mol\,kWh^{-1}\,d^{-1}$	References
Petit Saut	French Guiana	tropical	350	115	102	0.7	310.43	2.13	Guerin et al. (2006)
Balbina	Brazil	tropical	2360	250	76	2.1	717.44	19.82	Guerin et al. (2006)
Samuel	Brazil	tropical	540	216	976	5	2440.00	12.50	Guerin et al. (2006)
Tucurui	Brazil	tropical	2850	8370	237.11	12.01	80.74	4.09	Santos et al. (2006)
Itaipu	Brazil	tropical	1350	14000	27.39	0.78	2.64	0.08	Santos et al. (2006)
Laforge 1	Canada	boreal	1288	878	46.86	1.71	2.51	68.74	Tremblay et al. (2005)
Laforge 2	Canada	boreal	260	319	18.93	0.47	0.38	15.43	Tremblay et al. (2005)
La Grande 3	Canada	boreal	2420	2418	38.80	0.51	0.51	38.83	Tremblay et al. (2005)
La Grande 4	Canada	boreal	765	2779	26.77	0.68	0.19	7.37	Tremblay et al. (2005)
Robert-Bourassa	Canada	boreal	2835	5616	38.77	0.49	0.25	19.57	Tremblay et al. (2005)
F.D.Roosevelt	United States	temperate	306	6809	−9.89	0.14	−0.44	0.01	Soumis et al. (2004)
Dworshak	United States	temperate	37	400	−23.41	0.21	−2.17	0.02	Soumis et al. (2004)
Wallula	United States	temperate	157	1120	−9.48	0.53	−1.33	0.07	Soumis et al. (2004)
Shasta	United States	temperate	77	629	31.02	0.69	3.80	0.08	Soumis et al. (2004)
Lokka	Finland	boreal	417	1849*	35	2.1	0.47	7.89	Huttunen et al. (2003)
TGR	China	subtropical	1084	22500	96.18	0.32	4.63	0.02	This study

* Estimated from annual production of Lokka reservoir (675 GWh).

BGD
9, 14503–14535, 2012

Table 3. Emissions by thermal-power plant when generating power output equivalent to that of the Three Gorges power station in 2010.

Fuels	Emission factor retrieval from EFDB, IPCC 1997 ($tC\,MWh^{-1}$)	Efficiency (Graus et al., 2007) (%)	Emissions[a] (tC)	% of other energy sources
TGR	–	–	411 491	–
Natural gas	0.05508	44	10 561 590	3.9
Diesel oil	0.07272	34	18 045 254	2.3
Fuel oil	0.07596	34	18 849 251	2.2
Coal	0.09288	33	23 746 320	1.7

[a] Emissions equals capacity equivalent with the Three Gorges power station × emission factor / fuel efficiency (DosSantos et al., 2006).

BGD
9, 14503–14535, 2012

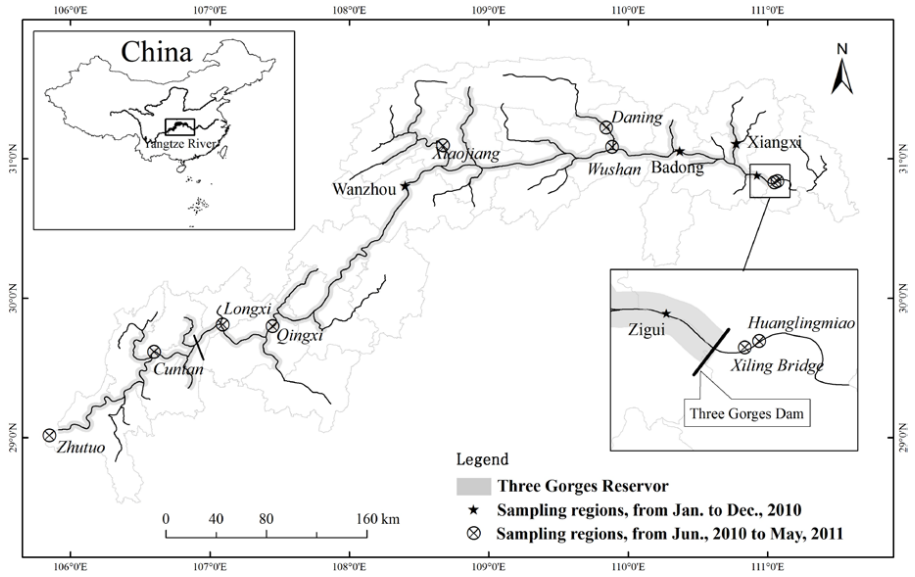

Fig. 1. Location of the Three Gorges Reservoir and all sampling sites.

BGD
9, 14503–14535, 2012

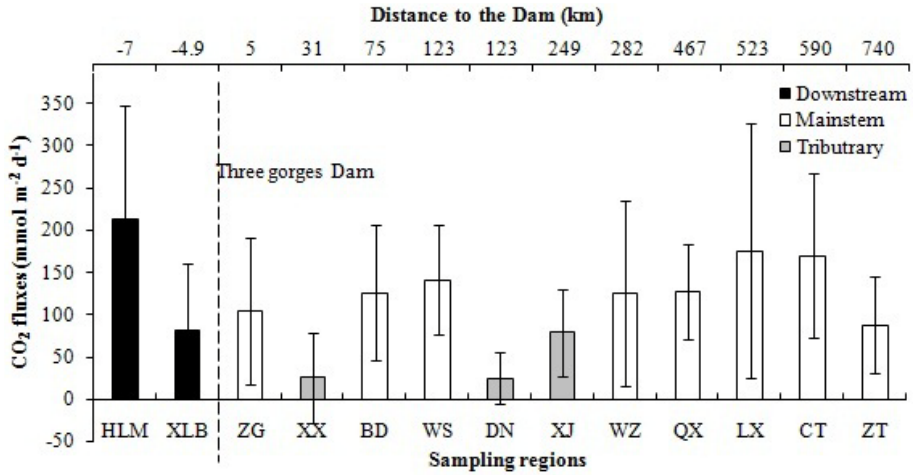

Fig. 2. Annual average CO_2 fluxes from different sampling sites of TGR. The dash line demonstrated the location of the Three Gorges Dam and all the sampling sites are arranged according to their distance to the dam (see the axis on the top). For the sampled tributaries (XX, DN and XJ) distance between the dam and tributary estuaries are used. Error bars indicated standard deviations. Annually, CO_2 flux at all the sites showed large variations with large standard deviation and flux at tributary sites show relatively lower values.

BGD
9, 14503–14535, 2012

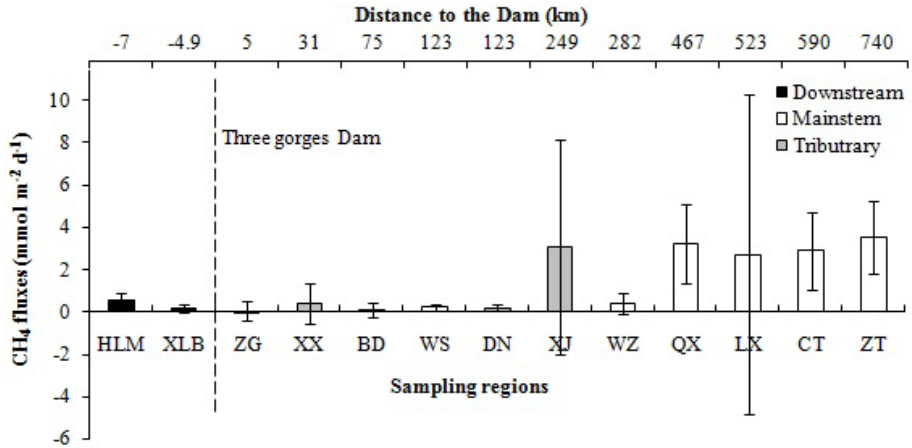

Fig. 3. Annual average CH_4 fluxes from different sampling sites of TGR. Error bars indicated the standard deviation. CH_4 fluxes at upper reach at mainstream (QX, LX, CT and ZT) are higher than other parts of the reservoir, while tributary sites (like XJ and XX) show relative higher fluxes.

BGD
9, 14503–14535, 2012

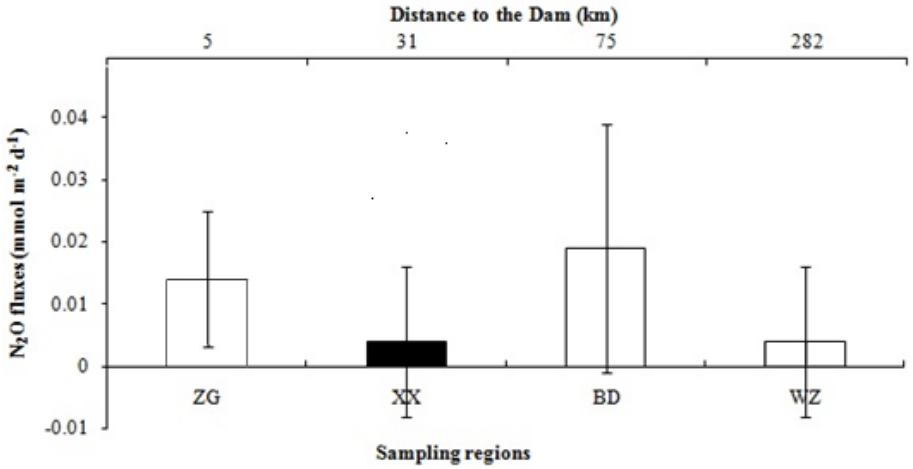

Fig. 4. Annual average N_2O fluxes from the four primary sampling regions of TGR. Basically fluxes at the three mainstream sites (white bars) are higher than tributary site of Xiangxi (XX, black bar).

BGD
9, 14503–14535, 2012

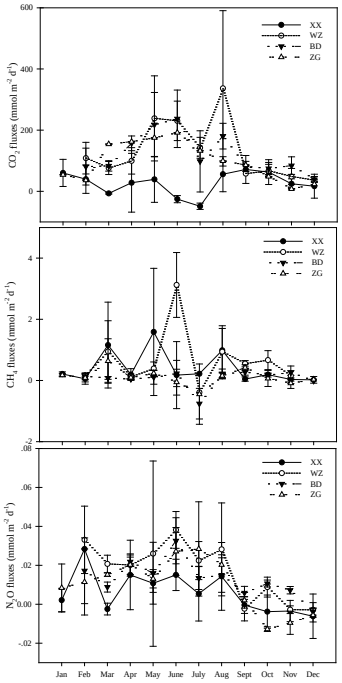

Fig. 5. Monthly variations of GHG fluxes from the four primary sampling sites. Each site have made 4 to 5 measurements to consider the great spatial variation of GHG fluxes and the error bars indicated the standard deviations which partly quantified these variations. CO_2 fluxes at mainstream sites (Zigui: ZG, Badong: BD, Wanzhou: WZ) have similar changing trend while the monthly variation in the tributary of Xiangxi (XX) is totally different in warm season due to the absorption of algae in Xiangxi River; changing trend of N_2O fluxes are more or less like the CO_2 fluxes at mainstream, indicating that there may be some common parameters influencing these two gas emissions; CH_4 have a more complex temporal variation indicating more complicated processes and parameters are involved.

BGD
9, 14503–14535, 2012

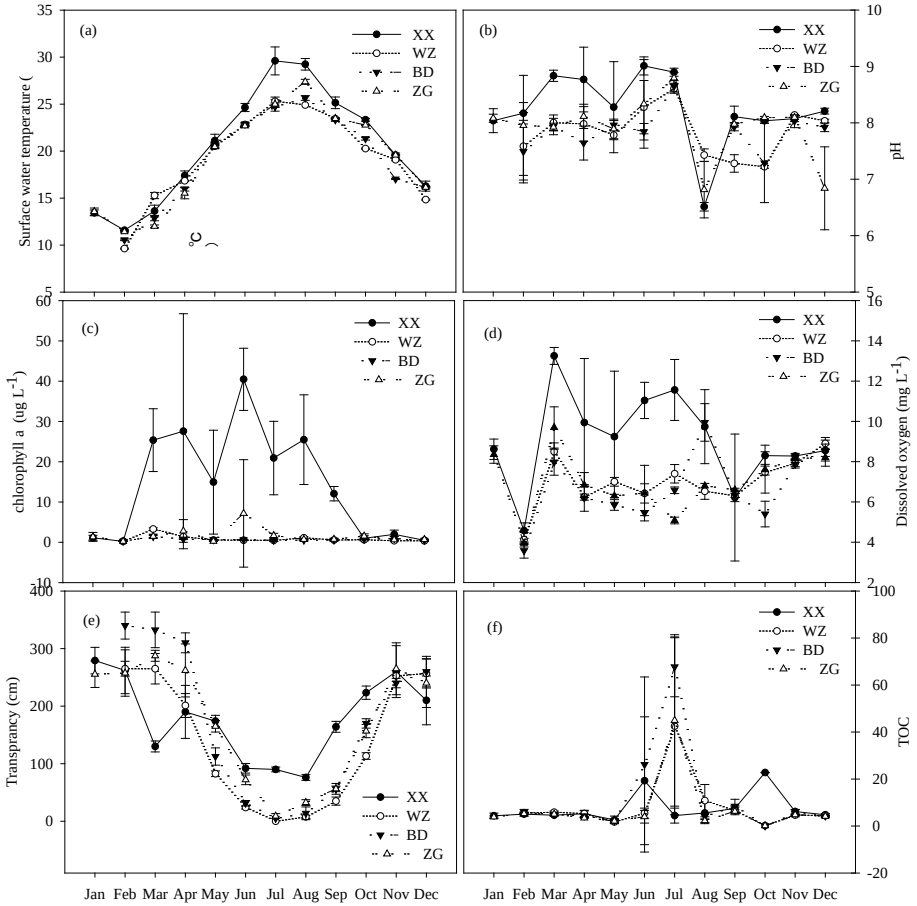

Fig. 6. Monthly variation of water quality parameters, from January to December, 2010.

BGD
9, 14503–14535, 2012

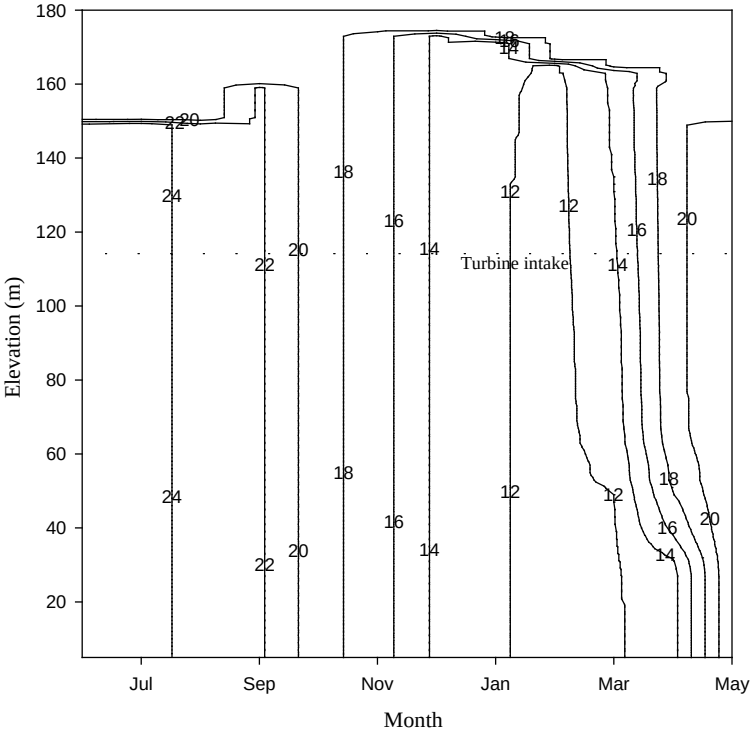

Fig. 7. Temperature profile at Three Gorges Dam region, from July 2008 to June 2009. The horizontal dotted line indicates the bottom of the turbine intake (116 m a.s.l., 15 m high and 9.5 m wide). During most time of the year water in this area is well mixed and there is no obvious stratification except at April and May. This phenomenon happens at most part of the reservoir, especially at the mainstream, mainly due to the deep discharge of the dam and water interchange between the mainstream and tributaries.

BGD
9, 14503–14535, 2012

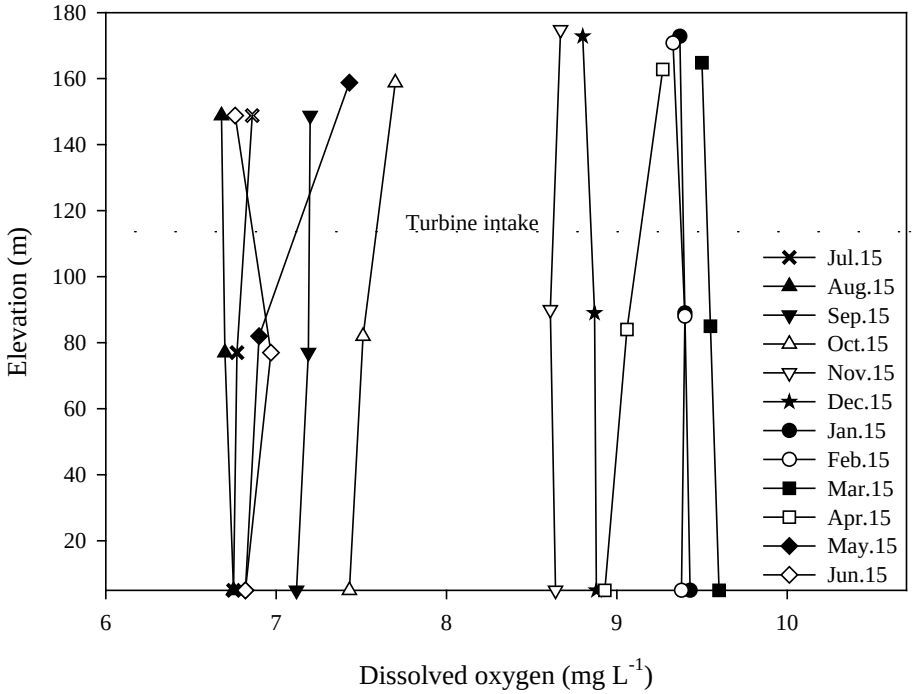

Fig. 8. Monthly variation of DO concentrations at surface water (0.2 m), bottom layer (0.5 m above the sediment) and the middle layer, from July 2008 to June 2009. The high DO concentration even at bottom of the reservoir is again approved that there are no significant stratification at these regions.

BGD
9, 14503–14535, 2012